

To be submitted to
Physical Review

UCRL-19569
Preprint

c 23

COMBINED ZEEMAN AND STARK EFFECT IN THE HYPERFINE
STRUCTURE OF THE $6^2P_{3/2}$ STATE OF THALLIUM
205 AND THE $4^2P_{3/2}$ STATE OF GALLIUM 69

RECEIVED
LAWRENCE
RADIATION LABORATORY

Joseph Yellin

SEP 16 1970

March 1970

LIBRARY AND
DOCUMENTS SECTION

AEC Contract No. W-7405-eng-48

TWO-WEEK LOAN COPY

*This is a Library Circulating Copy
which may be borrowed for two weeks.
For a personal retention copy, call
Tech. Info. Division, Ext. 5545*

LAWRENCE RADIATION LABORATORY
UNIVERSITY of CALIFORNIA BERKELEY

UCRL-19569
c 23

DISCLAIMER

This document was prepared as an account of work sponsored by the United States Government. While this document is believed to contain correct information, neither the United States Government nor any agency thereof, nor the Regents of the University of California, nor any of their employees, makes any warranty, express or implied, or assumes any legal responsibility for the accuracy, completeness, or usefulness of any information, apparatus, product, or process disclosed, or represents that its use would not infringe privately owned rights. Reference herein to any specific commercial product, process, or service by its trade name, trademark, manufacturer, or otherwise, does not necessarily constitute or imply its endorsement, recommendation, or favoring by the United States Government or any agency thereof, or the Regents of the University of California. The views and opinions of authors expressed herein do not necessarily state or reflect those of the United States Government or any agency thereof or the Regents of the University of California.

COMBINED ZEEMAN AND STARK EFFECT IN THE HYPERFINE STRUCTURE OF THE
 $6^2P_{3/2}$ STATE OF THALLIUM 205 AND THE $4^2P_{3/2}$ STATE OF GALLIUM 69*

Joseph Yellin

Lawrence Radiation Laboratory
University of California
Berkeley, California 94720

March 1970

ABSTRACT

The hyperfine structure of the $6^2P_{3/2}$ state of ^{205}Tl and the $4^2P_{3/2}$ state of ^{69}Ga is investigated in the presence of static electric and magnetic fields of arbitrary orientation. The emphasis is on low field level crossings which occur within the $F = 2$ hyperfine state of thallium and the $F = 3$ hyperfine state of gallium. Results of computer calculations for different relative orientations of the fields are presented and the influence of small off-axis fields on the level crossings is explored. The possibility of observing "anti-level crossing" by the atomic beam method is considered in an attempt to explain some anomalous experimental results.

I. INTRODUCTION

During the course of an investigation of the Stark effect in the resonance lines of indium by the atomic beam method, anomalous signals independent of the light were observed. These signals were found to depend on both the static magnetic and electric fields in the C-region of the atomic beam apparatus. Similar signals were later observed in gallium. It was subsequently learned that F. R. Petersen¹ had also observed anomalous signals during the course of an investigation of the tensor polarizability of the metastable $6^2P_{3/2}$ state of thallium and the $4^2P_{3/2}$ metastable state of gallium. The anomalous signals were characterized by the fact that they were independent of the exciting radiation (light in our case, radio frequency signals in Petersen's case) and depended only on the static electric and magnetic fields present in the C-region. Further evidence suggested that the signals originated in the $2^2P_{3/2}$ state rather than the $2^2P_{1/2}$ state. For example, the anomalous gallium signals were more intense than the anomalous indium signals while no anomalous thallium signals were observed by us. Now, the populations of the $2^2P_{3/2}$ states of thallium, indium, and gallium are approximately 0, 15% and 45% respectively for the atomic beam source temperature used. Hence one would expect greater signals for gallium than for indium and no signal for thallium if indeed the signals are associated with the $2^2P_{3/2}$ state.²

The fact that the anomalous signals depend on both the electric and magnetic fields suggests that some sort of level crossing phenomena may be involved with transitions taking place between the crossing levels.

Yet, the Zeeman and Stark operators are diagonal in the magnetic quantum numbers when the fields are parallel, so that no transitions can be induced in the absence of further perturbations. Additional perturbations may be provided by accidental off-axis components of the static fields. These facts have prompted us to investigate the combined Zeeman and Stark effects on the hyperfine structure of the $^2P_{3/2}$ states of thallium and gallium when the electric field is not parallel to the magnetic field. Indium will not be treated here since the tensor polarizability of indium has not been measured.

II. THEORY

To calculate the hyperfine structure of the $^2P_{3/2}$ it is necessary to diagonalize the Hamiltonian which consists of the hyperfine, Zeeman, and Stark operators. Each of these operators has been amply discussed in the literature.³ Thallium has a nuclear spin $I = 1/2$ and hence the hyperfine structure operator contains only the magnetic dipole term

$$\mathcal{H}^{hf} = \frac{a}{h} \underline{I} \cdot \underline{J} = a \frac{F(F+1) - I(I+1) - J(J+1)}{2h}$$

where the hyperfine constant $a = 530.076600$ MHz (^{205}Tl). \mathcal{H}^{hf} is diagonal in the Fm representation and it is convenient for our purposes to calculate the matrix elements of all operators in this representation. In most experiments involving both magnetic and electric fields, the fields are parallel and it is frequently simpler to work in the m_I, m_J representation since the Stark and Zeeman operators are diagonal in m_J, m_I . Here we are interested in the circumstance that \underline{E} is not parallel to \underline{B} . In this case, depending on which direction we choose for the z-axis either the Zeeman or the Stark operator will contain off-diagonal matrix elements. It is not clear that anything is to be gained by working in the m_I, m_J representation, particularly since the matrix elements will ultimately be calculated by computer.

The Zeeman operator is given by

$$\mathcal{H}^Z = -g_J \frac{\mu_0}{h} \underline{J} \cdot \underline{H} - g_I \frac{\mu_0}{h} \underline{I} \cdot \underline{H}$$

where $g_J (^{205}\text{Tl}) = -1.3341045$, and $g_I (^{205}\text{Tl}) = 0.0017549$, and where μ_0 is the Bohr magneton. We choose for the z-axis the direction of the magnetic field. The required matrix elements are then,

$$\langle F'm' | \mathcal{H}^Z | Fm \rangle = -g_J \frac{\mu_0}{h} H \langle F'm' | J_z | Fm \rangle - g_I \frac{\mu_0}{h} H \langle F'm' | I_z | Fm \rangle$$

Using the Wigner-Eckart theorem and the theorem for the reduced matrix element of a tensor operator in a coupled scheme we obtain⁴

$$\begin{aligned} \langle F'm' | \mathcal{H}^Z | Fm \rangle &= \frac{-\mu_0}{h} H (-)^{F'+I+J+1-m} [(2F+1)(2F'+1)]^{1/2} \begin{pmatrix} F' & 1 & F \\ -m & 0 & m \end{pmatrix} \\ &\times \left[(-)^F g_J [(2J+1) J(J+1)]^{1/2} \begin{Bmatrix} J & F' & I \\ F & J & 1 \end{Bmatrix} \right. \\ &\left. + (-)^{F'} g_I [(2I+1) I(I+1)]^{1/2} \begin{Bmatrix} I & F' & J \\ F & I & 1 \end{Bmatrix} \right] \end{aligned}$$

Substituting $I = 1/2$, $J = 3/2$, and evaluating the 3-j and 6-j symbols in terms of their arguments we get

$$\langle F+1m | \mathcal{H}^Z | Fm \rangle = GH \left[\frac{(F)(F+2)(F+4)(2-F)}{(F+1)^2(2F+1)(2F+3)} \right]^{1/2} [(F+1)^2 - m^2]^{1/2} \quad \text{and}$$

$$\langle Fm | \mathcal{H}^Z | Fm \rangle = -GH \frac{3m}{F(F+1)} - G'Hm \quad \text{where}$$

$$G = \frac{\mu_0}{2h} (-g_J + g_I) \quad \text{and} \quad G' = \frac{\mu_0}{2h} (g_J + g_I)$$

These matrix elements are given in Table I.

The matrix elements of the Stark operator in the Fm representation have been given by Angel and Sanders,⁵

$$\begin{aligned} \langle F'm' | \mathcal{H}^E | Fm \rangle &= -\frac{\sqrt{6}}{4} \alpha_2 \sum_Q (-)^Q \{EE\}_{-Q}^2 (-)^{F-m} \begin{pmatrix} F & 2 & F' \\ -m & Q & m' \end{pmatrix} \\ &(-)^{I+J+F} \left[\frac{(2F+1)(2F'+1)(2J+3)(2J+2)(2J+1)}{2J(2J-1)} \right]^{1/2} \begin{Bmatrix} J & F & I \\ F' & J & 2 \end{Bmatrix} \end{aligned}$$

where α_2 is the tensor polarizability⁶

$$\left(\alpha_2(Tl) = -6.04 \text{ kHz} / \left(\frac{\text{kV}}{\text{cm}} \right)^2 \right), \quad \text{where}$$

$$\{EE\}_{-Q}^2 = \sqrt{5} \sum_{qq'} (-)^Q \begin{pmatrix} 1 & 1 & 2 \\ q & q' & Q \end{pmatrix} E_q E_{q'} \quad \text{and where}$$

$$E_{\pm 1} = \mp \frac{1}{\sqrt{2}} (E_x \pm iE_y), \quad E_0 = E_z. \quad \text{It is of interest to calculate}$$

the matrix elements for the two limiting cases when \underline{E} is parallel to \underline{B} and when \underline{E} is perpendicular to \underline{B} . An examination of these cases will tell us which states are coupled by the electric field.

Case I. \underline{E} is parallel to \underline{B} .

In this case $|\underline{E}| = E_z$ and $Q = 0$. Hence, $m = m'$, i.e. only diagonal (in m) matrix elements exist. We have,

$$\{EE\}_0^2 = \frac{2}{\sqrt{6}} E_z^2 \quad \text{and thus}$$

$$\langle F'm' | \mathcal{H}^E | Fm \rangle = -\sqrt{5} \alpha_2 (-)^{2F-m} \begin{pmatrix} F & 2 & F' \\ -m & 0 & m \end{pmatrix} \begin{Bmatrix} 3/2 & F & 1/2 \\ F' & 3/2 & 2 \end{Bmatrix} \\ [(2F+1)(2F'+1)]^{1/2} E_z^2.$$

These matrix elements are shown in Table II.

Case II. \underline{E} perpendicular to \underline{B} .

In this case, $|\underline{E}| = E_x$, $E_{\pm 1} = \mp \frac{1}{\sqrt{2}} E_x$, $E_0 = 0$. Hence,

$$\{EE\}_{\pm 2}^2 = \frac{1}{2} E_x^2$$

$$\{EE\}_{\pm 1}^2 = 0$$

$$\{EE\}_0^2 = \frac{1}{\sqrt{6}} E_x^2$$

From this it is seen that the electric field couples states whose magnetic quantum numbers differ by 2. The matrix elements for this case are given in Table III. The general case we are interested in is that in which the electric field is in the X-Z plane. Here the coupling between the Zeeman sublevels will vary from maximum at 90° to zero at 0° . For angles other than 0° or 90° levels whose magnetic quantum numbers differ by ± 1 are also coupled. In Table IV matrix elements for 45° are given.

The matrix elements for gallium may be worked out similarly except that \mathcal{H}^{hf} must include the electric quadrupole interaction. In our calculations we have included also the magnetic octupole interaction.

We have chosen the direction of the magnetic field as the axis of quantization. We could just as well have taken the direction of the electric field as the axis of quantization. The results are the same in either case. We can go from one choice of axis to the other by a rotation of the coordinate axis and this cannot effect the physical results.

A computer program was written to calculate the energies of the hyperfine sublevels as a function of both the magnitude and relative orientation of the electric field. The results of these computations are discussed in Section IV. In the next section we discuss an illuminating and relevant example.

III. EXAMPLE

The features of the combined Zeeman Stark effect for the case that \underline{E} is not parallel to \underline{H} will be considered here through a simple example. We consider a state with $J = 1, I = 0$ (no hyperfine structure). The operators for this case are

$$\mathcal{H}^Z = -g_J \mu_0 H J_z \quad \text{and} \quad \mathcal{H}^E = \frac{-1}{2} \alpha_2 \frac{3J_z^2 - J(J+1)}{J(2J-1)} E^2$$

for \underline{E} parallel to \underline{H} . Hence,

$$\langle m' | \mathcal{H} | m \rangle = \begin{matrix} m' & m & -1 & 0 & +1 \\ \begin{matrix} -1 \\ 0 \\ +1 \end{matrix} & \begin{pmatrix} -2\epsilon + \beta & 0 & 0 \\ 0 & 4\epsilon & 0 \\ 0 & 0 & -2\epsilon - \beta \end{pmatrix} \end{matrix} \quad \text{where } \beta = g_J \mu_0 H$$

and $\epsilon = 1/4 \alpha_2 E^2$. Here we see that the energies are simply the sum of the Zeeman and Stark energies. \mathcal{H}^E for the case that \underline{E} is perpendicular to \underline{H} can be obtained most easily by use of the rotation operator

$$\langle m' | \mathcal{H}^E | m \rangle_\phi = (D_{m', \bar{m}}^1(\phi))^{-1} \langle \bar{m} | \mathcal{H}^E | \bar{m}' \rangle D_{\bar{m}', m}^1(\phi)$$

$$\begin{matrix} m' & m & -1 & 0 & 1 \\ \begin{matrix} -1 \\ 0 \\ 1 \end{matrix} & \begin{pmatrix} -\epsilon(3 \cos^2 \phi - 1) & 3\sqrt{2} \epsilon \sin \phi \cos \phi & -3 \epsilon \sin^2 \phi \\ 3\sqrt{2} \epsilon \sin \phi \cos \phi & 2 \epsilon(3 \cos^2 \phi - 1) & -3\sqrt{2} \epsilon \sin \phi \cos \phi \\ -3 \epsilon \sin^2 \phi & -3\sqrt{2} \epsilon \sin \phi \cos \phi & -\epsilon(3 \cos^2 \phi - 1) \end{pmatrix} \end{matrix}$$

For $\phi = \pi/2$ we have

$$\langle m' | \mathcal{H} | m \rangle = \begin{matrix} m' & \begin{matrix} m & -1 & 0 & 1 \end{matrix} \\ \begin{matrix} -1 \\ 0 \\ 1 \end{matrix} & \begin{pmatrix} \epsilon + \beta & 0 & -3\epsilon \\ 0 & -2\epsilon & 0 \\ -3\epsilon & 0 & \epsilon - \beta \end{pmatrix} \end{matrix}$$

The eigenvalues of \mathcal{H} are readily shown to be $\lambda = -2\epsilon, \epsilon \pm 3\epsilon(1 + \delta^2)^{1/2}$ where $\delta = \beta/3\epsilon$. Here we see that the fields no longer act independently. The electric field in this case tries to restore the Stark degeneracy removed by the magnetic field. The two situations described above are shown in Figs. 1(a) and (d). We note that the crossing point in Fig. 1(a) has disappeared in Fig. 1(d) and that the shapes of the energy curves labeled $m = 0, -1$ in Fig. 1(a) have reversed in Fig. 1(d). We now examine more carefully what happens at the crossing point when a small perpendicular electric field component exists, that is we consider the case when $\phi(\text{rad}) \ll 1$. Making the approximation $\sin \phi \approx \phi, \cos \phi \approx 1$ we have

$$\langle m' | \mathcal{H} | m \rangle = \langle m' | \mathcal{H}^Z | m \rangle + \langle m' | \mathcal{H}^E | m \rangle_{\phi \ll 1}$$

$$\begin{matrix} m' & \begin{matrix} m & -1 & 0 & 1 \end{matrix} \\ \begin{matrix} -1 \\ 0 \\ 1 \end{matrix} & \begin{pmatrix} \frac{2}{3}\beta & \frac{\sqrt{2}}{2}\beta\phi & 0 \\ \frac{\sqrt{2}}{2}\beta\phi & \frac{2}{3}\beta & -\frac{\sqrt{2}}{2}\beta\phi \\ 0 & \frac{\sqrt{2}}{2}\beta\phi & -\frac{4}{3}\beta \end{pmatrix} \end{matrix}$$

where we have used the fact that $\epsilon = \beta/6$ at the crossing point. $\langle m' | \mathcal{H} | m \rangle$ can be broken up into two parts,

$$\langle m' | \mathcal{H}_0 | m \rangle = \begin{matrix} m' & m & -1 & 0 & 1 \\ & \swarrow & & & \\ -1 & \left(\begin{array}{cccc} \frac{2}{3} \beta & 0 & 0 & 0 \\ 0 & +\frac{2}{3} \beta & 0 & 0 \\ 0 & 0 & 0 & -\frac{4}{3} \beta \end{array} \right) & & & \\ 1 & & & & \end{matrix}$$

and $\langle m' | \mathcal{H}' | m \rangle = \begin{matrix} m' & m & -1 & 0 & 1 \\ & \swarrow & & & \\ -1 & \left(\begin{array}{cccc} 0 & \frac{\sqrt{2}}{2} \beta \phi & 0 & 0 \\ \frac{\sqrt{2}}{2} \beta \phi & 0 & -\frac{\sqrt{2}}{2} \beta \phi & 0 \\ 0 & \frac{\sqrt{2}}{2} \beta \phi & 0 & 0 \end{array} \right) & & & \\ 1 & & & & \end{matrix}$

Applying degenerate perturbation theory to \mathcal{H}' we get $\pm 1/\sqrt{2} \beta \phi$ as the correction to the energies of the degenerate states $|0\rangle$ and $|-1\rangle$. Thus the degeneracy is lifted by an amount $\sqrt{2} \beta \phi$ and the result is that the crossing becomes "anti-crossing". This is shown in Fig. 1(b) and (c). In the example just given, the degeneracy at the crossing is lifted in first order as the crossing levels are directly coupled with $\phi \neq \pi/2$. More generally, the crossing levels may or may not be coupled in first order. Since the Stark operator connects levels whose m values differ by one or two we can expect that crossings by such levels would be removed in first order, whereas for $\Delta m > 2$ the levels are coupled in higher order. Thus we can expect that directly coupled levels would be very sensitive to a misalignment of \underline{E} while others would be less sensitive.

The above example gives us a very good idea of what to expect for the $F = 1$ hyperfine state of thallium and gallium. The hyperfine structure

splittings in both cases is very much larger than the combined Zeeman Stark effect we wish to consider and hence to a very good approximation we may neglect perturbations due to the other hyperfine states. The operators then assume the form

$$\mathcal{H}^Z = - g_F \mu_0 H F_z$$
$$\mathcal{H}^S = - \frac{1}{2} \alpha_2 \frac{3F_z^2 - F(F+1)}{F(2F-1)} E_z^2$$

and this is just the case treated above.⁷ In the calculations that follow no approximations were made, rather the entire Hamiltonian was diagonalized.

IV. RESULTS AND DISCUSSION

Calculations for ^{205}Tl and ^{69}Ga were performed for a fixed magnetic field of 0.2-0 gauss and 0.100 gauss respectively. Tensor polarizabilities measured by Petersen were used. The scalar polarizability shifts all levels by the same amount and hence is irrelevant. The matrix elements were calculated by machine for each value of the electric field in increments of 0.5 kV and the Hamiltonian $\mathcal{H} = \mathcal{H}^{\text{hf}} + \mathcal{H}^{\text{S}} + \mathcal{H}^{\text{Z}}$ diagonalized. Calculations were repeated for different angles. The results are shown in Figs. 2-5. Of particular interest are the $\Delta m = \pm 1$ crossings since these levels are strongly coupled. We note that each crossing point turns into an "anti-crossing" as the field is rotated. Nine crossings occur in the $F = 3$ state of ^{69}Ga for which $\Delta m = 1, 2, 3, 4,$ or 5 . In the thallium $F = 2$ state four crossings occur with $\Delta m = 1, 2,$ or 3 . Since the Stark operator couples directly levels for which $\Delta m = 1$ or 2 when $\phi \neq 0$ we can expect that crossings between levels m and $m + 1$ or m and $m + 2$ will be removed in first order, as in the example of the last section, while for $\Delta m > 2$ the degeneracy will be removed in second or higher order. We can estimate the sensitivity of a crossing to the field alignment when $\Delta m = 1$ or 2 and $\phi(\text{rad}) \ll 1$. We have in this case $E_{\pm 1} \cong \pm \frac{1}{\sqrt{2}} E \phi$, $E_0 = E$ and thus,

$$\sum_{qq'} \begin{pmatrix} 1 & 1 & 2 \\ qq' & \pm 1 & \end{pmatrix} E_q E_{q'} = \mp \frac{2}{\sqrt{10}} E^2 \phi$$

$$\sum_{qq'} \begin{pmatrix} 1 & 1 & 2 \\ qq' & \pm 2 & \end{pmatrix} E_q E_{q'} = \frac{1}{2\sqrt{5}} E^2 \phi^2$$

Substituting these results into the matrix element of the Stark operator we obtain

$$\begin{aligned} \langle F_{m+1} | \mathcal{H}^S | F_m \rangle &= \pm \sqrt{15} (-1)^{I+J+F} \begin{Bmatrix} 3/2 & F & I \\ F & 3/2 & 2 \end{Bmatrix} (-1)^{F-m} \begin{pmatrix} F & 2 & F \\ -m & \pm 1 & m \mp 1 \end{pmatrix} \\ &\quad \times (2F+1) \alpha_2 E^2 \phi \\ \langle F_{m+2} | \mathcal{H}^S | F_m \rangle &= -\frac{\sqrt{30}}{4} (-1)^{I+J+F} \begin{Bmatrix} 3/2 & F & I \\ F & 3/2 & 2 \end{Bmatrix} (-1)^{F-m} \begin{pmatrix} F & 2 & F \\ -m & \pm 2 & m \mp 2 \end{pmatrix} \\ &\quad \times (2F+1) \alpha_2 E^2 \phi^2. \end{aligned}$$

We now apply degenerate perturbation theory as in the example of Section III.

The result is that the degeneracy is removed by

$$\epsilon' = \begin{cases} 2 |\langle F_{m+1} | \mathcal{H}^S | F_m \rangle| & |\Delta m| = 1 \\ 2 |\langle F_{m+2} | \mathcal{H}^S | F_m \rangle| & |\Delta m| = 2 \end{cases}$$

Specializing to the $F = 2$ state of thallium we get

$$\begin{aligned} \epsilon' &= |(1+2m)[(3+m)(2-m)]^{1/2} \frac{1}{2\sqrt{2}} \alpha_2 E_0^2 \phi|, \quad |\Delta m| = 1 \\ \epsilon' &= [(1-m)(2-m)(3+m)(4+m)]^{1/2} \frac{1}{8} \alpha_2 E_0^2 \phi^2|, \quad |\Delta m| = 2 \end{aligned}$$

and for the $F = 3$ state of gallium

$$\begin{aligned} \epsilon' &= |(1+2m)[(4+m)(3-m)]^{1/2} \frac{\sqrt{2}}{10} \alpha_2 E_0^2 \phi|, \quad |\Delta m| = 1 \\ \epsilon' &= [(2-m)(3-m)(4+m)(5+m)]^{1/2} \frac{1}{20} \alpha_2 E_0^2 \phi^2|, \quad |\Delta m| = 2 \end{aligned}$$

where E_0 is the value of E at the crossing. Crossings for which $\Delta m = 2$ are seen to be less sensitive by a factor ϕ to the field alignment than are $\Delta m = 1$ crossings. Of special interest are the crossing between the $m = -2$ and $m = -1$ levels in gallium since transitions between them result in refocusing of the atomic beam. For this crossing we have,

$$\epsilon' = \frac{3}{\sqrt{5}} \alpha_2 E_0^2 \phi \quad \text{Ga} \quad \phi \ll 1$$

When we substitute E_0 from Fig. 4 we see that $\epsilon'(\text{Ga}) \approx 7 \text{ kHz/deg}$ for the $m = -1, m = -2$ crossing. Thus the field orientation is critical and would have a very serious effect on the results of radiofrequency experiments. For example, serious errors in the determination of α_2 by the atomic beam magnetic resonance method can occur if the fields are not parallel. We consider next how signals might arise at the crossing point in the absence of externally applied oscillations.

The perturbation due to the off-axis field strongly mixes levels m and $m+1$ in the vicinity of the crossing point and consequently transitions take place.⁸ The transition probability peaks at the crossing point where the wave function oscillates with frequency $\nu = \langle F_m | \mathcal{H} | F_{m+1} \rangle / \hbar \sim \alpha_2 E^2 \phi$ between the crossing levels. Such transitions, induced by static fields, are known from anti-level crossing experiments in excited states⁹ and should be observable in ground and low lying metastable states by the atomic beam method provided (1) transitions between the crossing levels lead to a refocused beam and (2) the transit time of an atom through the C-region $T \approx 1/\nu$. The last condition follows from the fact that the transition probability is appreciable only when the splitting between the anti-crossing levels is comparable to the width of the levels which is determined by the transit (interaction) time.

FOOTNOTES AND REFERENCES

* Work performed under the auspices of the U. S. Atomic Energy Commission.

1. F. R. Petersen (private communication).
2. The $^2P_{3/2}$ state of thallium was populated by optical pumping of the beam in Petersen's experiment.
3. N. F. Ramsey, Molecular Beams (Oxford University Press, London, 1956).
4. A. R. Edmond, Angular Momentum in Quantum Mechanics (Princeton University Press, 1957, Princeton).
5. J. R. P. Angel and P. G. H. Sandars, Proc. Roy. Soc. A305, 125 (1968).
6. G. Palmer, F. R. Petersen and R. C. Mockler, Bull. Am. Phys. Soc. 12, 905 (1967); F. R. Petersen, Bull. Am. Phys. Soc. 14, 833 (1969).
7. Note the relationship between $\alpha_2(F)$ and $\alpha_2(J)$ in Ref. 5.
8. For an elementary discussion of degenerate perturbations see Quantum Theory, by David Bohm (Prentice-Hall, Inc., 1951), Chapter 19.
9. T. G. Eck, L. L. Foldy and H. Wieder, Phys. Rev. Letters 10, 239 (1963); in this experiment the anti-crossing is caused by a hyperfine perturbation. For a discussion of anti-crossing see G. W. Series, Phys. Rev. Letters 11, 13 (1963); J. J. Forney and E. Geneux, Phys. Letters 20, 632 (1966); here a magnetic field is applied perpendicularly to an electric field and consequently levels for which $\Delta m = 2$ are coupled.

Table I. Matrix elements of the Zeeman operator for thallium. $G = \mu_0/h (-g_J + g_I)$ and $G' = \mu_0/2h (g_J + g_I)$.

		F=2					F=1			
		m								
		m'	-2	-1	0	1	2	-1	0	1
F'=2	-2	(2G'-G)H	0	0	0	0	0	0	0	0
	-1	0	$(G' - \frac{1}{2}G)H$	0	0	0	0	$-\frac{\sqrt{3}}{2}GH$	0	0
	0	0	0	0	0	0	0	0	GH	0
	1	0	0	0	$(-G' + \frac{1}{2}G)H$	0	0	0	0	$-\frac{\sqrt{3}}{2}GH$
	2	0	0	0	0	$(-2G'+G)H$	0	0	0	0
F'=1	-1	0	$-\frac{\sqrt{3}}{2}GH$	0	0	0	0	$(G' - \frac{3}{2}G)H$	0	0
	0	0	0	GH	0	0	0	0	0	0
	1	0	0	0	$-\frac{\sqrt{3}}{2}GH$	0	0	0	0	$(-G' + \frac{3}{2}G)H$

$$\langle F'm' | \mathcal{H}^Z | Fm \rangle =$$

Table II. Matrix elements of the Stark operator for thallium. The electric field is directed along the z-axis.

$$\langle F'm' | \mathcal{H}^E | Fm \rangle =$$

		F=2					F=1		
		m					m		
		-2	-1	0	1	2	-1	0	1
F'=2	-2	$-\frac{2}{\sqrt{5}} \epsilon$	0	0	0	0	0	0	0
	-1	0	$\frac{\epsilon}{\sqrt{5}}$	0	0	0	$\sqrt{3} \epsilon$	0	0
	0	0	0	$\frac{2\epsilon}{\sqrt{5}}$	0	0	0	0	0
	1	0	0	0	$\frac{\epsilon}{\sqrt{3}}$	0	0	0	$-\sqrt{3}\epsilon$
	2	0	0	0	0	$-\frac{2\epsilon}{\sqrt{5}}$	0	0	0
F'=1	-1	0	$\sqrt{3} \epsilon$	0	0	0	$-\frac{\epsilon}{\sqrt{3}}$	0	0
	0	0	0	0	0	0	0	0	0
	1	0	0	0	$-\sqrt{3}\epsilon$	0	0	0	$-\frac{\epsilon}{\sqrt{3}}$

Table III. Matrix elements of the Stark operator for thallium. The electric field is directed along the x-axis.

$$\langle F'm' | \mathcal{H}^E | Fm \rangle =$$

	m		m'
			-2
			-1
			0
			1
			2
			-1
			0
			1
			2
			-1
			0
			1
			2
			-1
			0
			1
			2
			-1
			0
			1
			2
			-1
			0
			1
			2
			-1
			0
			1
			2
			-1
			0
			1
			2
			-1
			0
			1
			2
			-1
			0
			1
			2
			-1
			0
			1
			2
			-1
			0
			1
			2
			-1
			0
			1
			2
			-1
			0
			1
			2
			-1
			0
			1
			2
			-1
			0
			1
			2
			-1
			0
			1
			2
			-1
			0
			1
			2
			-1
			0
			1
			2
			-1
			0
			1
			2
			-1
			0
			1
			2
			-1
			0
			1
			2
			-1
			0
			1
			2
			-1
			0
			1
			2
			-1
			0
			1
			2
			-1
			0
			1
			2
			-1
			0
			1
			2
			-1
			0
			1
			2
			-1
			0
			1
			2
			-1
			0
			1
			2
			-1
			0
			1
			2
			-1
			0
			1
			2
			-1
			0
			1
			2
			-1
			0
			1
			2
			-1
			0
			1
			2
			-1
			0
			1
			2
			-1
			0
			1
			2
			-1
			0

Table IV. Matrix elements of the Stark operator for thallium. The electric field is directed 45° to the z-axis.

$$\langle F'm' | \mathcal{H}^E | Fm \rangle =$$

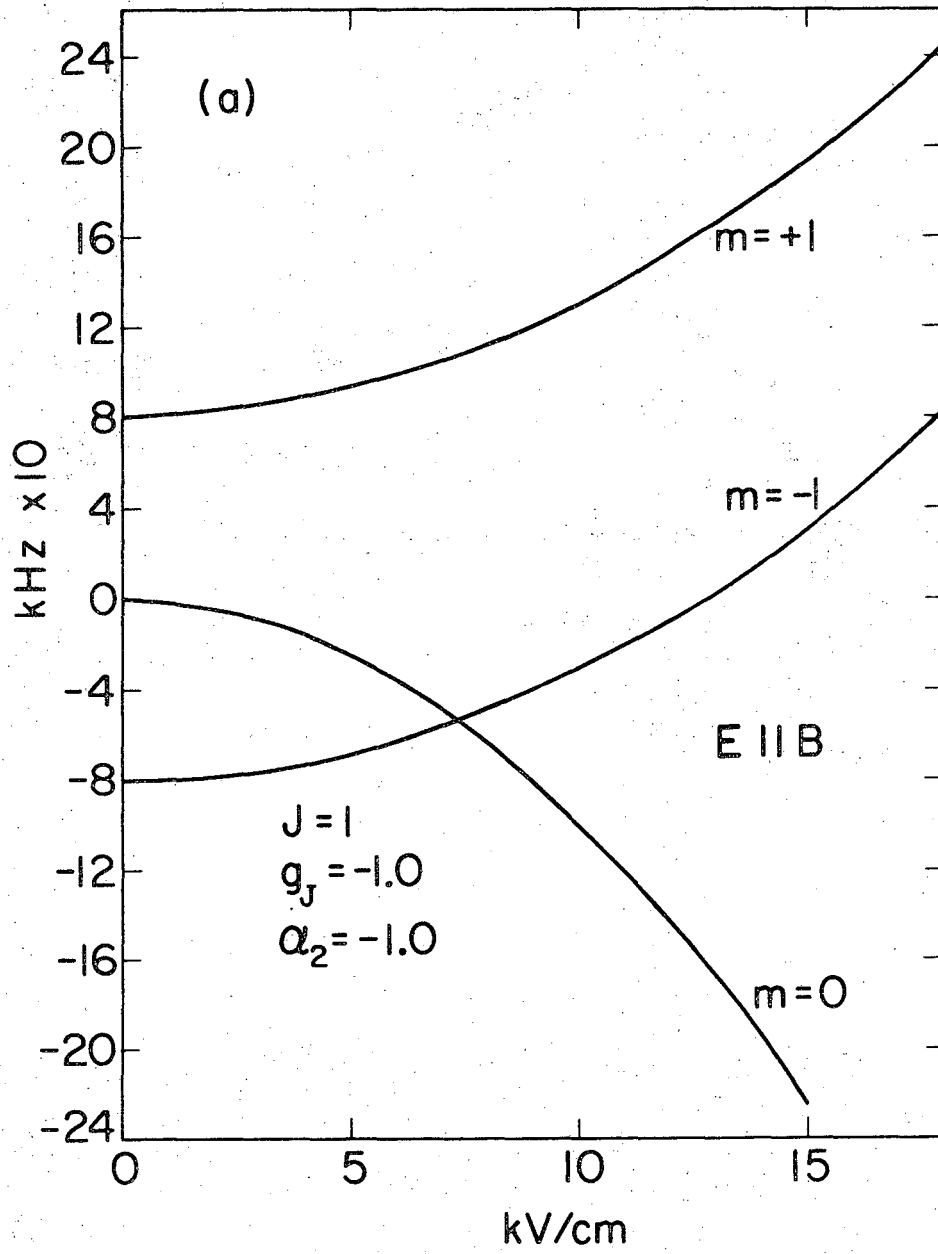
		F=2					F=1		
		-2	-1	0	1	2	-1	0	1
F'=2	m'	-2	-1	0	1	2	-1	0	1
	-2	$-\frac{1}{2} \epsilon$	$\frac{3}{2} \epsilon$	$-\frac{\sqrt{6}}{4} \epsilon$	0	0	$-\frac{\sqrt{3}}{2} \epsilon$	$\frac{\sqrt{6}}{4} \epsilon$	0
	-1	$\frac{3}{2} \epsilon$	$\frac{1}{4} \epsilon$	$\frac{\sqrt{6}}{4} \epsilon$	$-\frac{3}{4} \epsilon$	0	$-\frac{3}{4} \epsilon$	$\frac{\sqrt{6}}{4} \epsilon$	$\frac{\sqrt{3}}{4} \epsilon$
	0	$-\frac{\sqrt{6}}{4} \epsilon$	$\frac{\sqrt{6}}{4} \epsilon$	$\frac{1}{2} \epsilon$	$-\frac{\sqrt{6}}{4} \epsilon$	$-\frac{\sqrt{6}}{4} \epsilon$	$\frac{3\sqrt{2}}{4} \epsilon$	0	$\frac{3\sqrt{2}}{4} \epsilon$
	1	0	$-\frac{3}{4} \epsilon$	$-\frac{\sqrt{6}}{4} \epsilon$	$\frac{1}{4} \epsilon$	$-\frac{3}{2} \epsilon$	$-\frac{\sqrt{3}}{4} \epsilon$	$\frac{\sqrt{6}}{4} \epsilon$	$\frac{\sqrt{3}}{4} \epsilon$
	2	0	0	$-\frac{\sqrt{6}}{4} \epsilon$	$-\frac{3}{2} \epsilon$	$-\frac{1}{2} \epsilon$	0	$-\frac{\sqrt{6}}{4} \epsilon$	$-\frac{\sqrt{3}}{2} \epsilon$
	-1	$-\frac{\sqrt{3}}{2} \epsilon$	$-\frac{\sqrt{3}}{4} \epsilon$	$\frac{3\sqrt{2}}{4} \epsilon$	$-\frac{\sqrt{3}}{4} \epsilon$	0	$-\frac{1}{4} \epsilon$	$\frac{3\sqrt{2}}{4} \epsilon$	$-\frac{3}{4} \epsilon$
	0	$\frac{\sqrt{6}}{4} \epsilon$	$\frac{\sqrt{6}}{4} \epsilon$	0	$\frac{\sqrt{6}}{4} \epsilon$	$-\frac{\sqrt{6}}{4} \epsilon$	$\frac{3\sqrt{2}}{4} \epsilon$	$\frac{1}{2} \epsilon$	$-\frac{3\sqrt{2}}{4} \epsilon$
	1	0	$\frac{3}{4} \epsilon$	$\frac{3\sqrt{2}}{4} \epsilon$	$\frac{\sqrt{3}}{4} \epsilon$	$-\frac{\sqrt{3}}{2} \epsilon$	$-\frac{3}{4} \epsilon$	$-\frac{3\sqrt{2}}{4} \epsilon$	$-\frac{1}{4} \epsilon$

$$\epsilon = \frac{1}{4} \alpha_2 E^2$$

FIGURE CAPTIONS

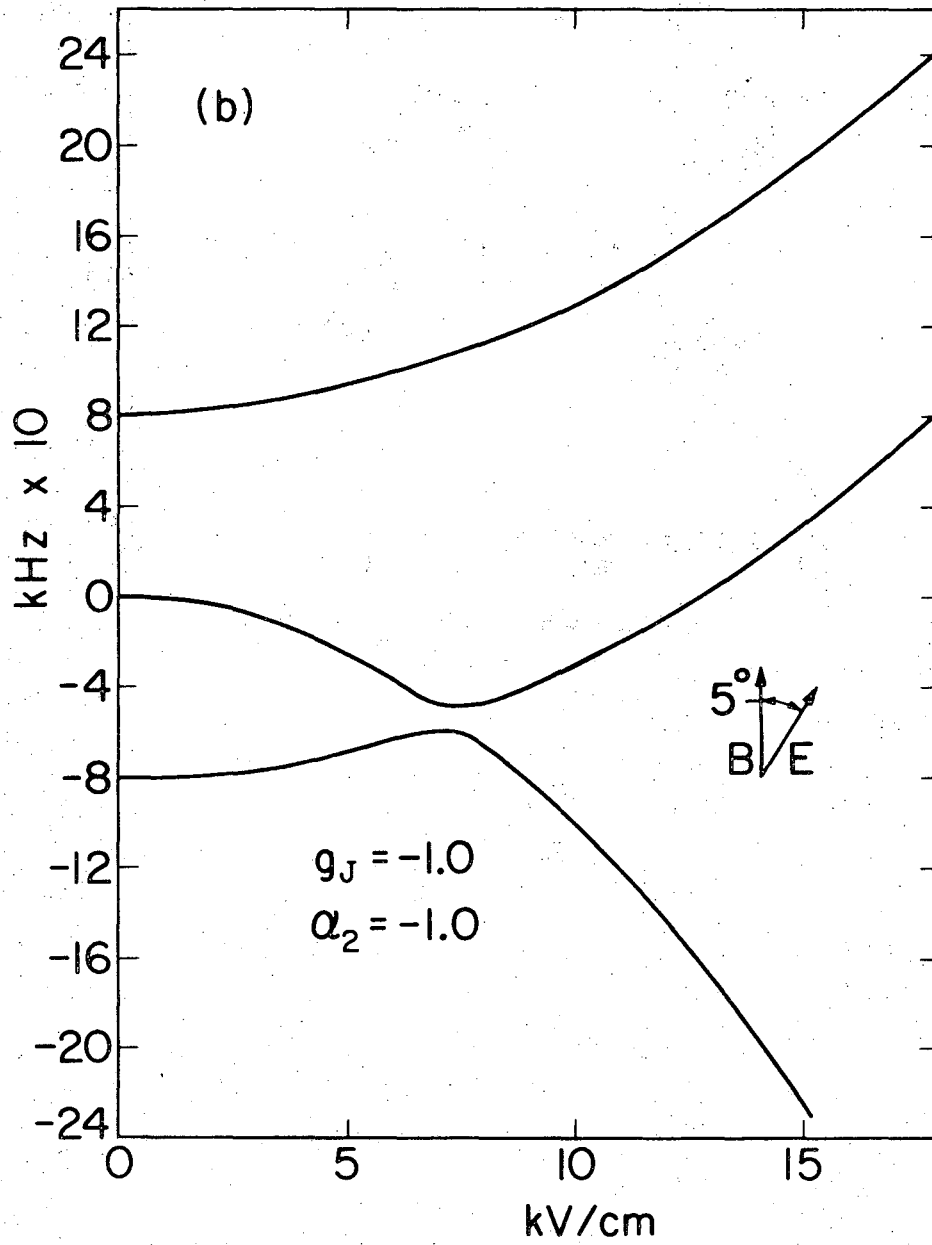
- Fig. 1. Combined Zeeman-Stark effect in a $J = 1$ state for different orientations of the electric field \underline{E} . The calculations were done for a magnetic field $B = 58$ milligauss with $g_J = -1$, $\alpha_2 = -1 \text{ kHz}/(\frac{\text{kV}}{\text{cm}})^2$. (a) \underline{E} parallel to \underline{B} . (b) \underline{E} makes a 5° angle with \underline{B} . (c) \underline{E} makes a 45° angle with \underline{B} . (d) \underline{E} is perpendicular to \underline{B} .
- Fig. 2. Combined Zeeman-Stark effect in the $F = 1 \ 6^2P_{3/2}$ state of ^{205}Tl . The magnetic field $B = 0.200$ gauss. (a) \underline{E} is parallel to \underline{B} . (b) \underline{E} makes a 15° angle with \underline{B} . (c) \underline{E} makes a 45° angle with \underline{B} . (d) \underline{E} makes a 90° angle with \underline{B} .
- Fig. 3. Combined Zeeman-Stark effect in the $F = 2 \ 6^2P_{3/2}$ state of ^{205}Tl . The magnetic field in $B = 0.200$ gauss. (a) \underline{E} is parallel to \underline{B} . (b) \underline{E} makes a 15° angle with \underline{B} . (c) \underline{E} makes a 45° angle with \underline{B} . (d) \underline{E} is perpendicular to \underline{B} .
- Fig. 4. Combined Zeeman-Stark effect in the $F = 3 \ 4^2P_{3/2}$ state of ^{69}Ga . The magnetic field $B = 0.100$ gauss. (a) \underline{E} is parallel to \underline{B} and \underline{E} makes a 5° angle with \underline{B} . (b) \underline{E} makes a 10° angle with \underline{B} and \underline{E} makes a 15° angle with \underline{B} . (c) \underline{E} is perpendicular to \underline{B} .
- Fig. 5. Combined Zeeman-Stark effect in the $F = 1 \ 4^2P_{3/2}$ state of ^{69}Ga . The magnetic field $B = 0.100$ gauss. (a) \underline{E} is parallel to \underline{B} and \underline{E} makes a 5° angle with \underline{B} . (b) \underline{E} makes a 10° angle with \underline{B} and \underline{E} makes a 15° angle with \underline{B} . (c) \underline{E} is perpendicular to \underline{B} .
- Fig. 6. Combined Zeeman-Stark effect in the $F = 2$ and $F = 0 \ 4^2P_{3/2}$ states of ^{69}Ga . The magnetic field is $B = 0.100$ gauss. The magnetic sublevels of the $F = 2$ hyperfine state have a very weak dependence on the electric field.

This is due to the vanishing of all matrix elements $\langle F=2, m_F | \mathcal{H}^S | F=2, m_F \rangle$ for the case that $I = 3/2$ and $J = 3/2$. The weak dependence comes from matrix elements non-diagonal in F .



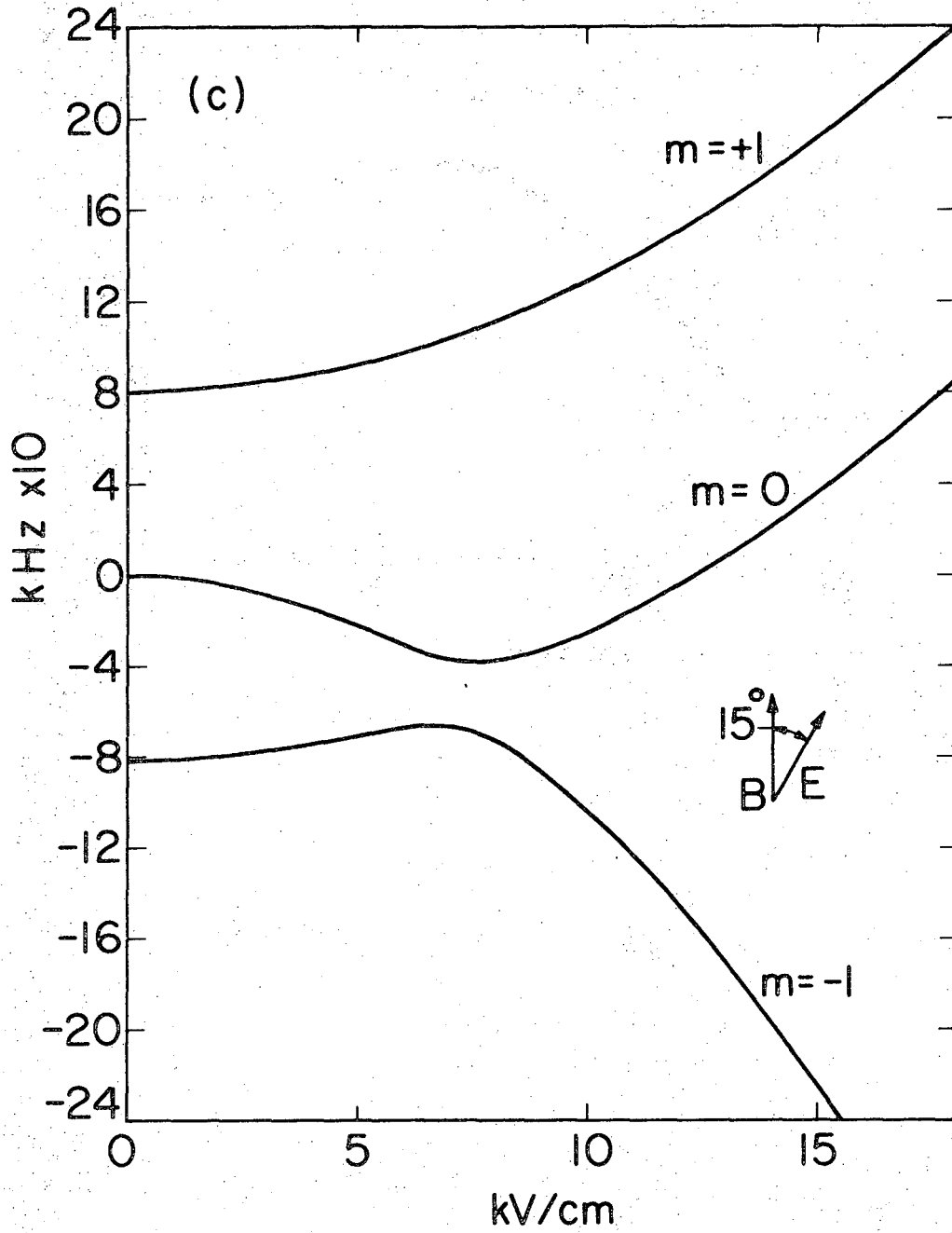
XBL703-2563

Fig. 1a



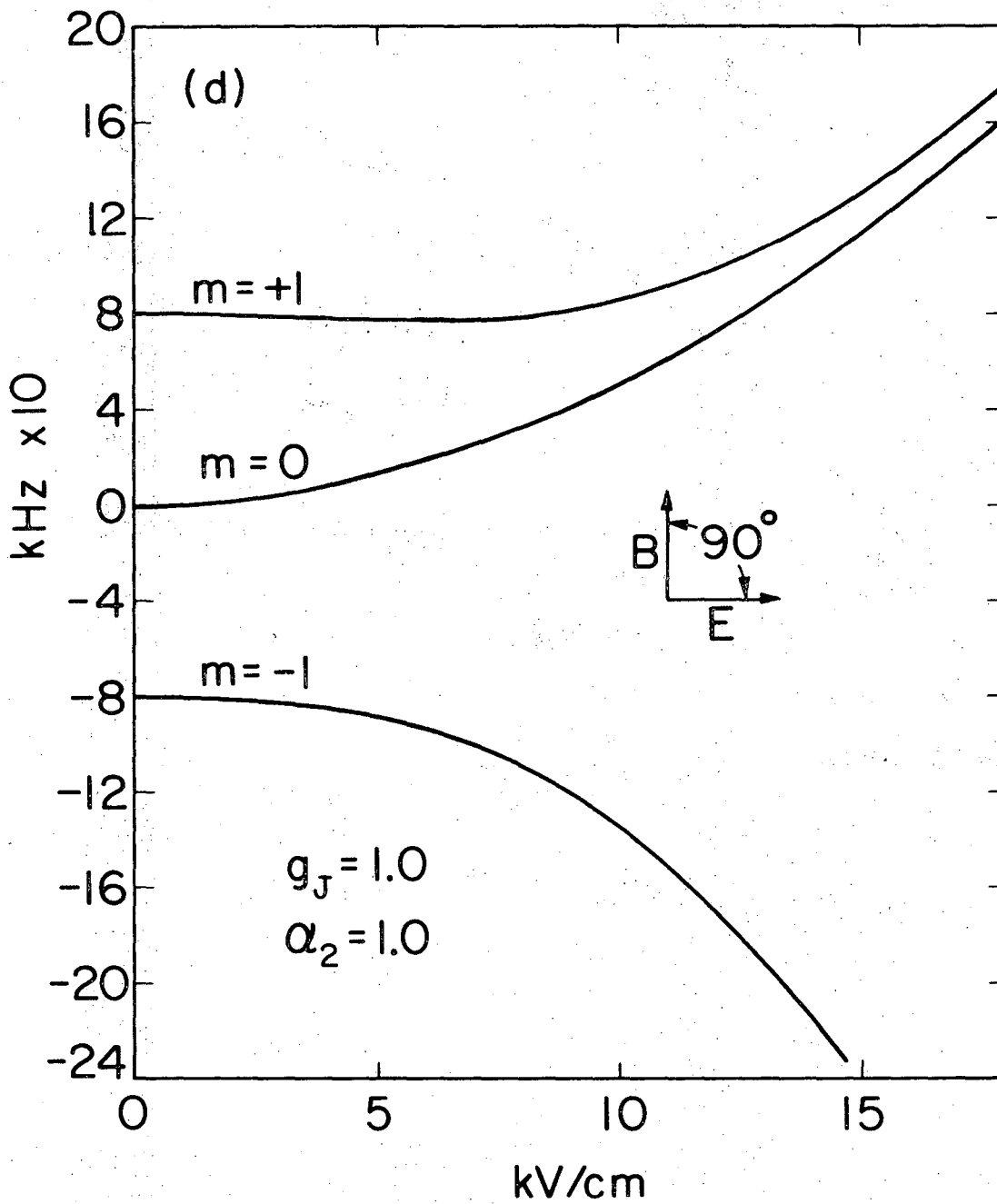
XBL703-2565

Fig. 1b



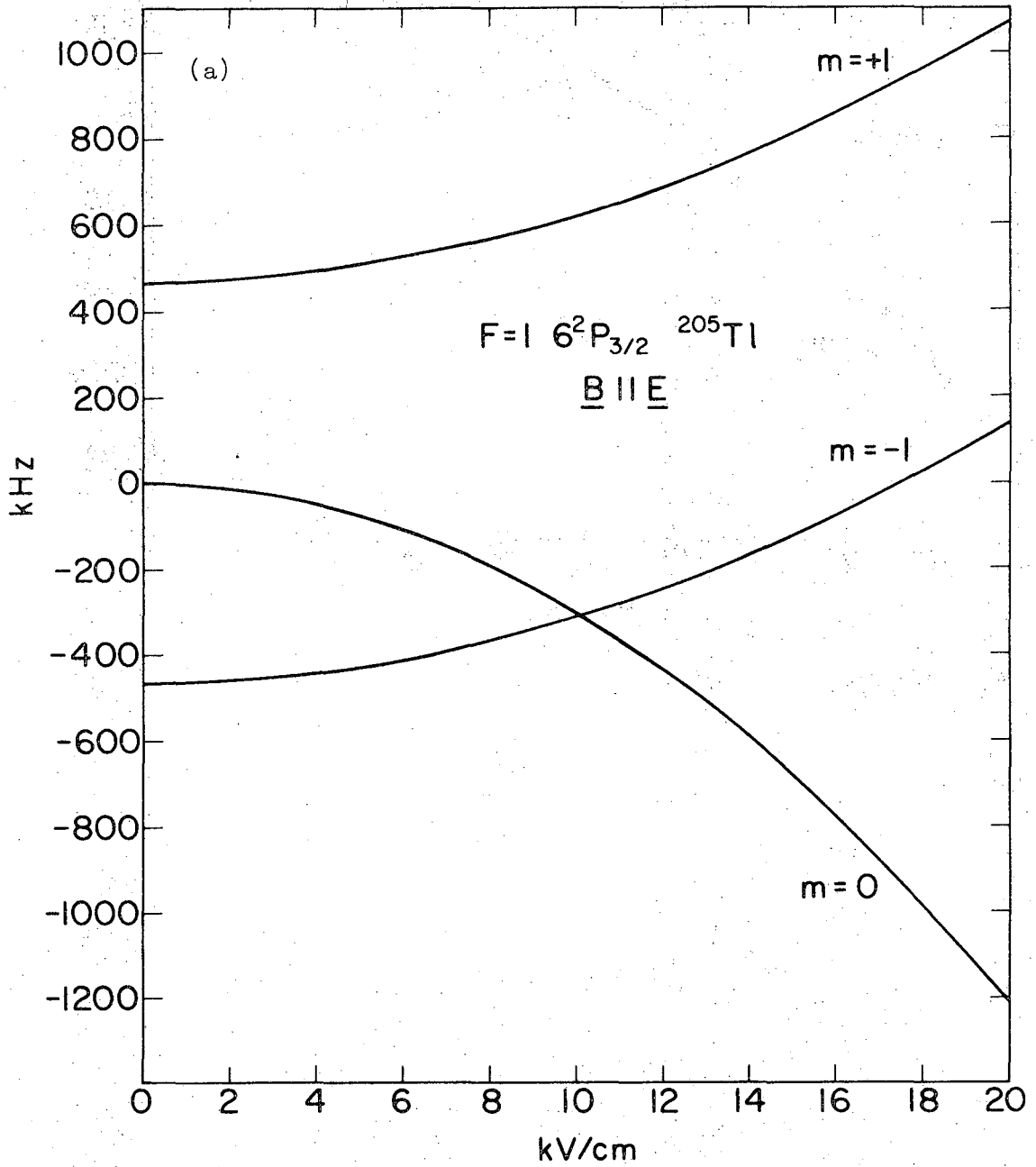
XBL703-2566

Fig. 1c



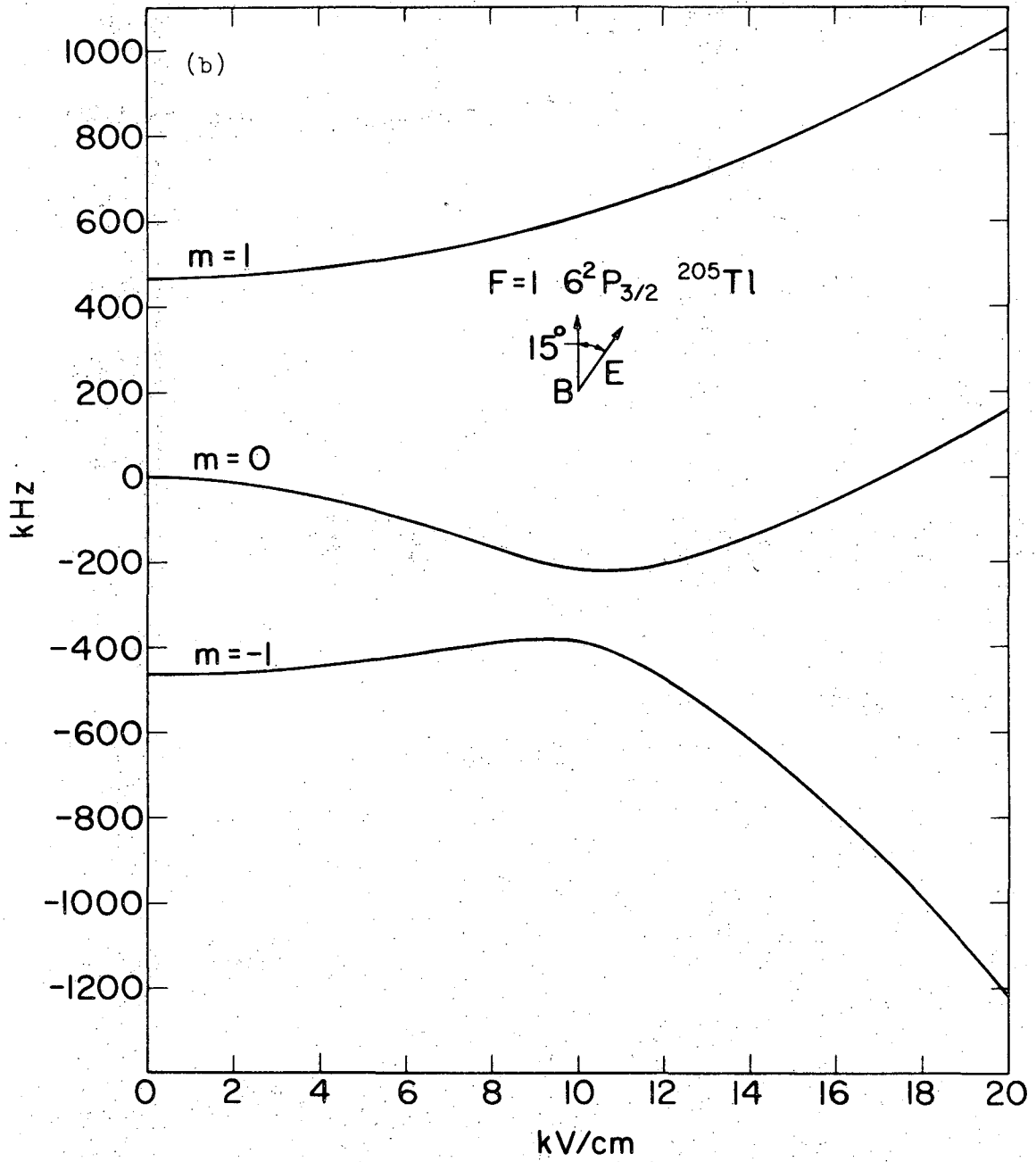
XBL703-2567

Fig. 1d



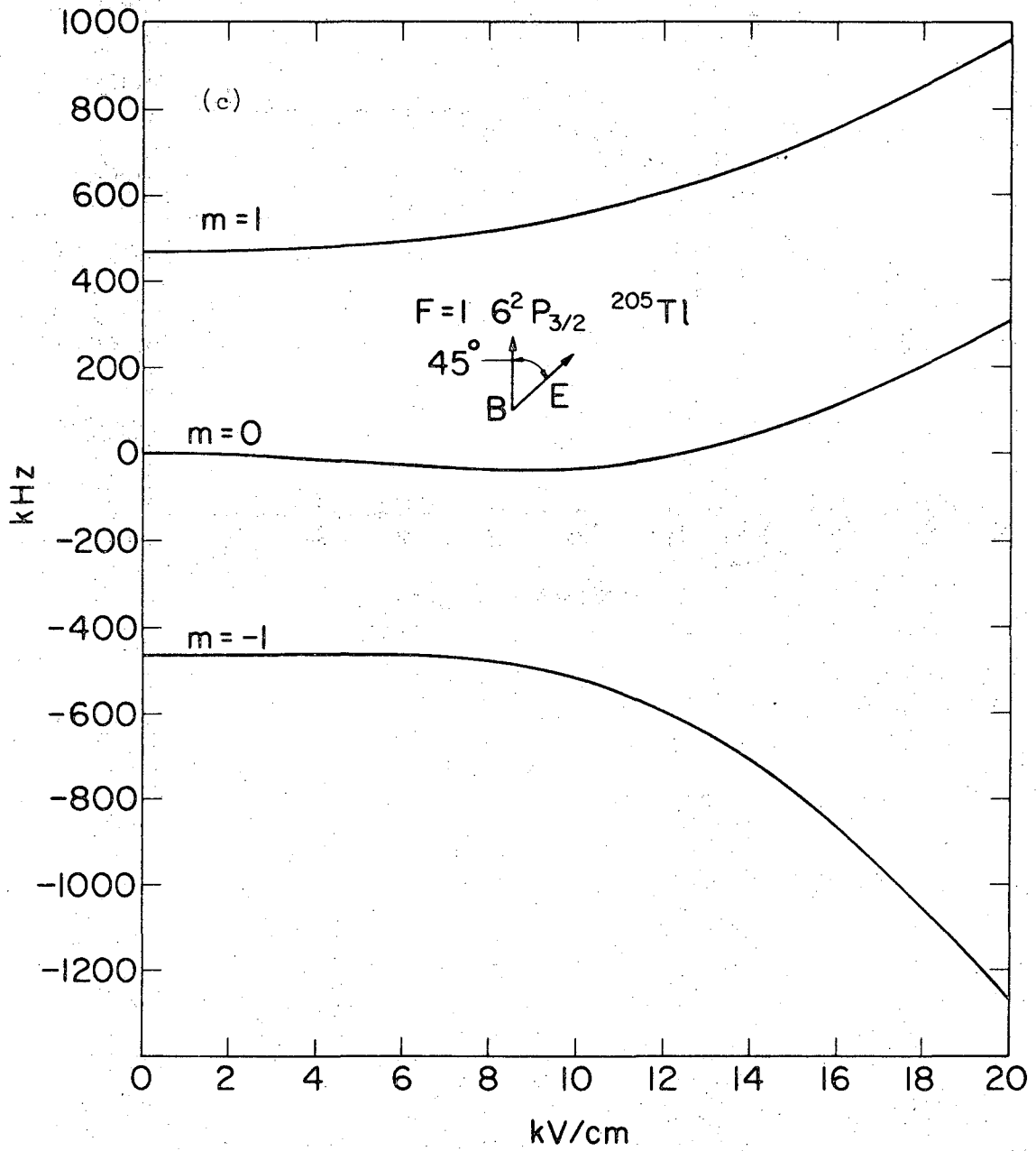
XBL703-2578

Fig. 2a



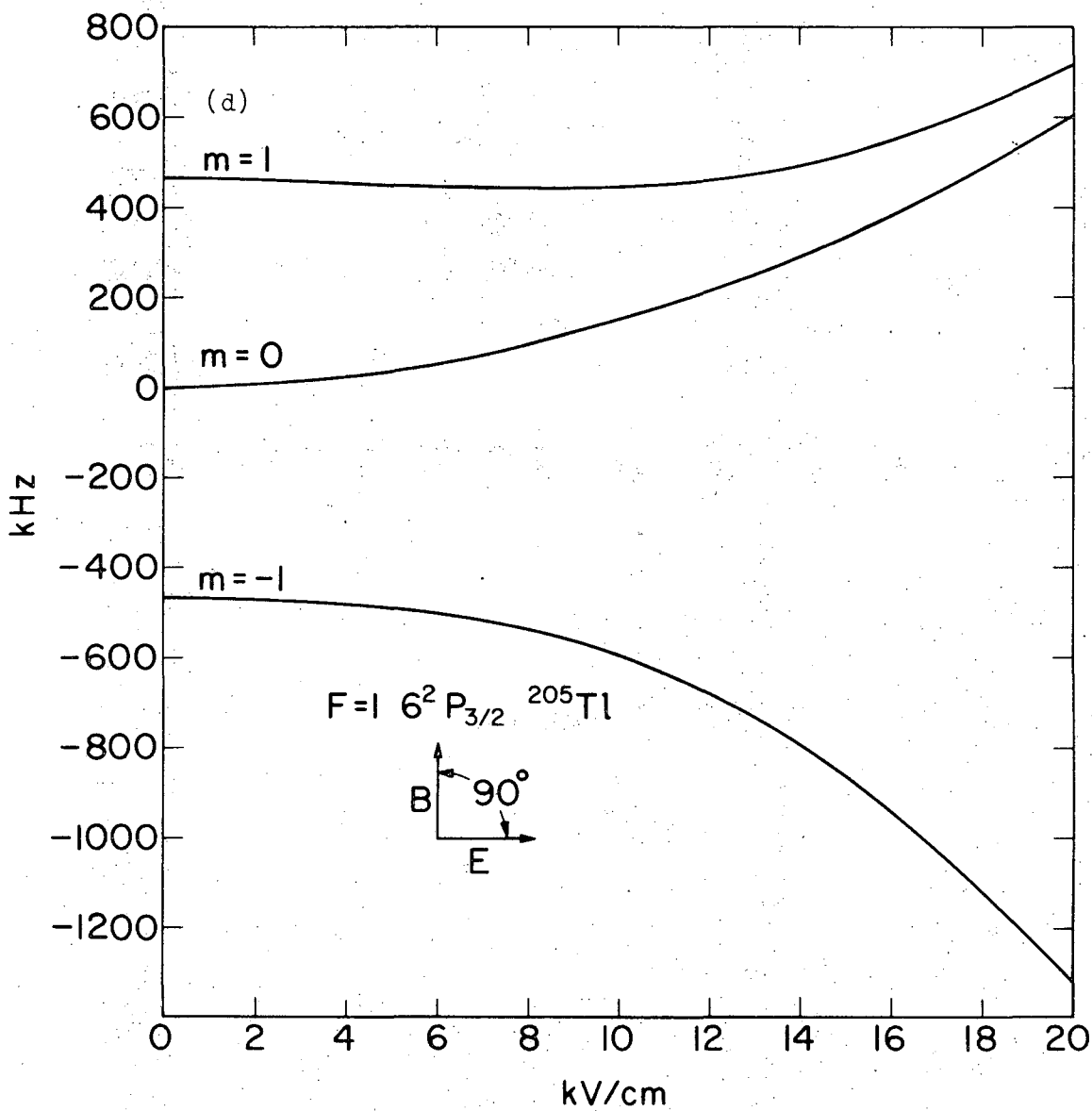
XBL703-2580

Fig. 2b



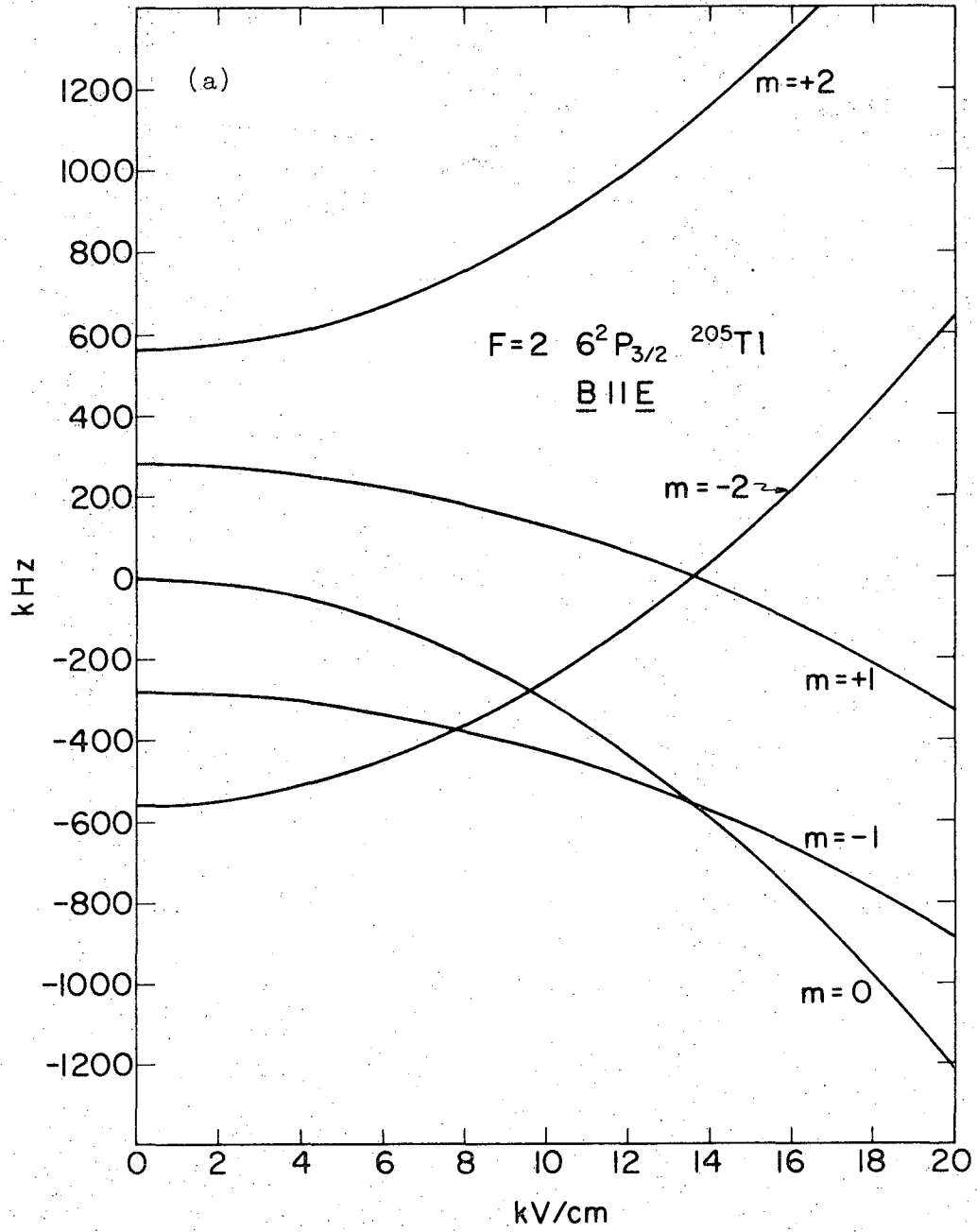
XBL703-2582

Fig. 2c



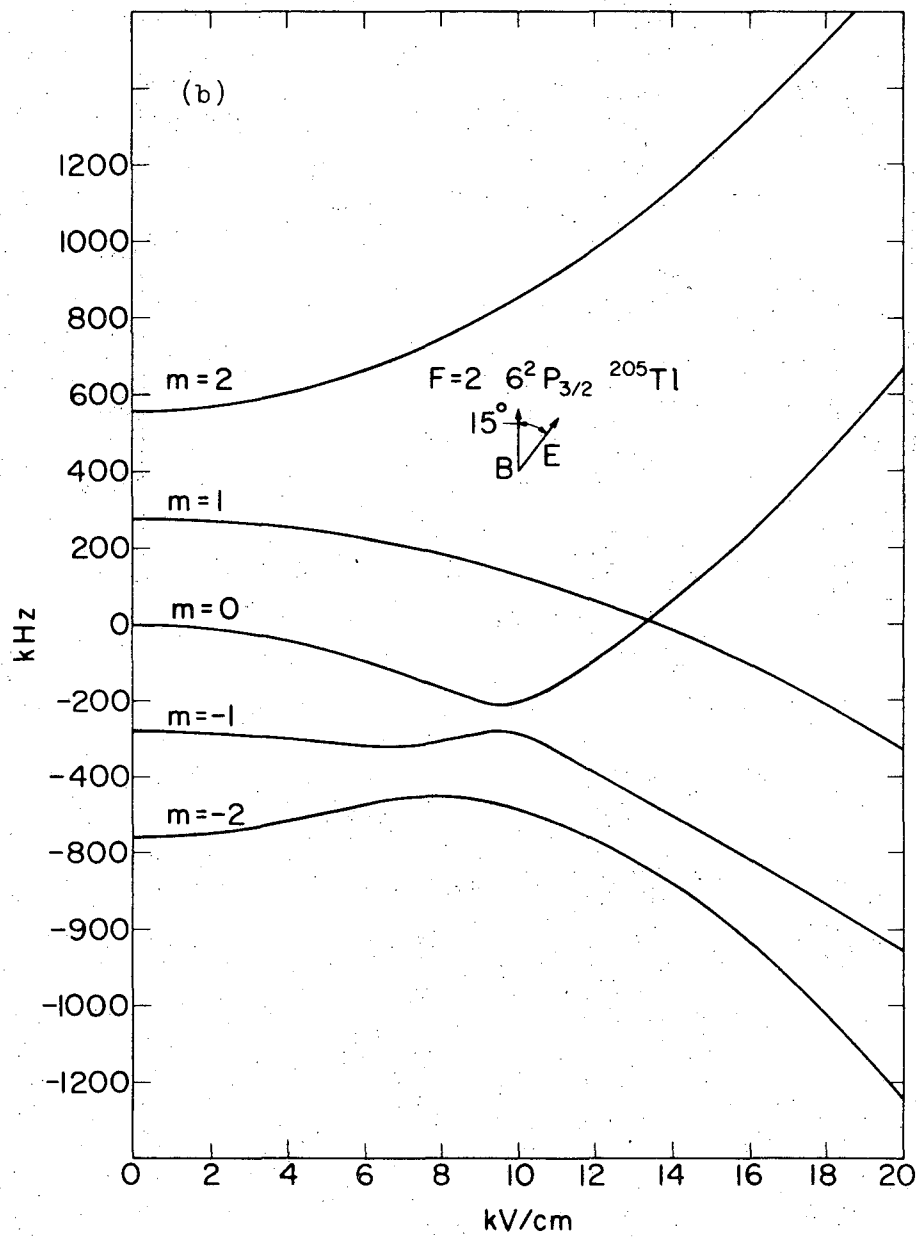
XBL703-2584

Fig. 2d



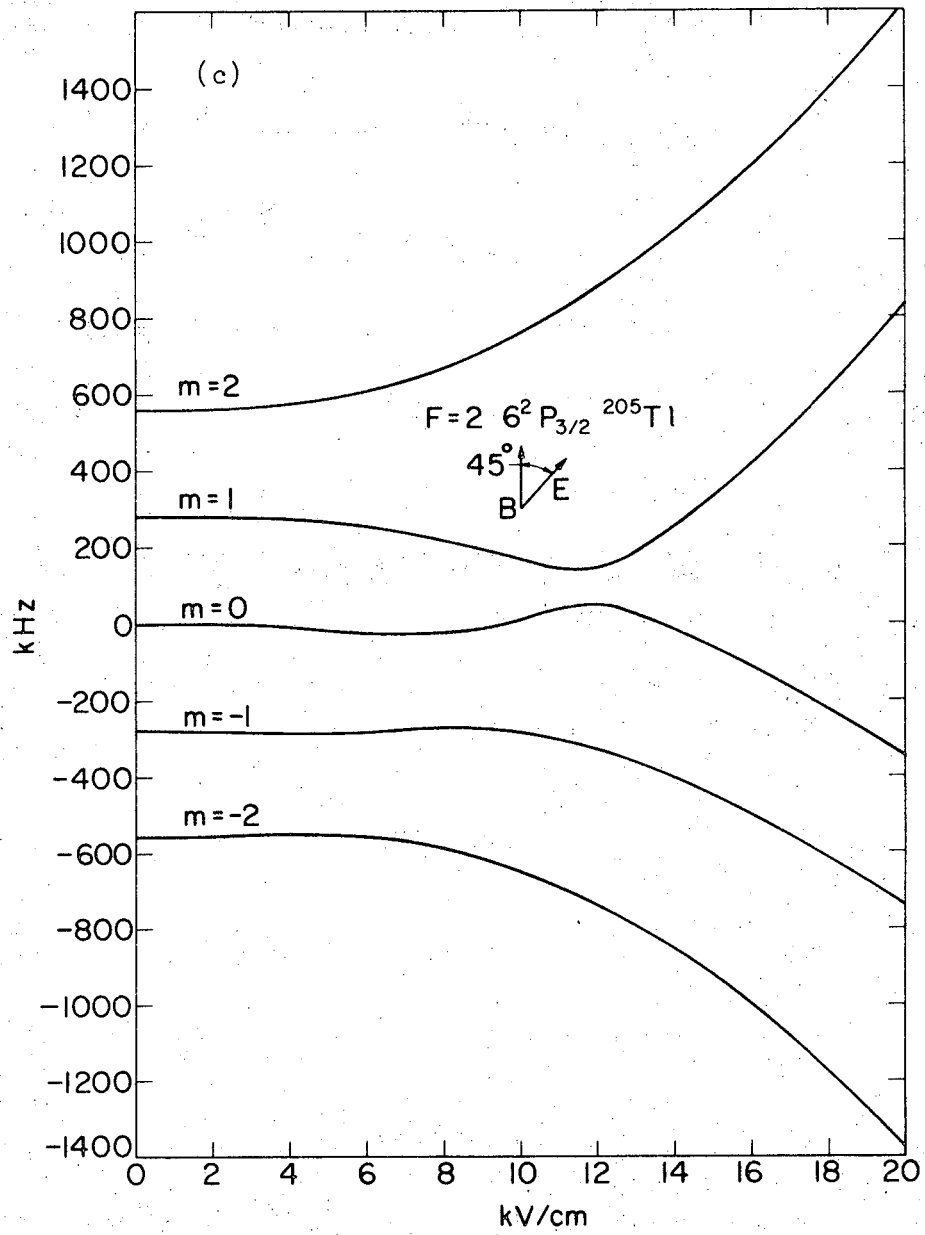
XBL703-2577

Fig. 3a



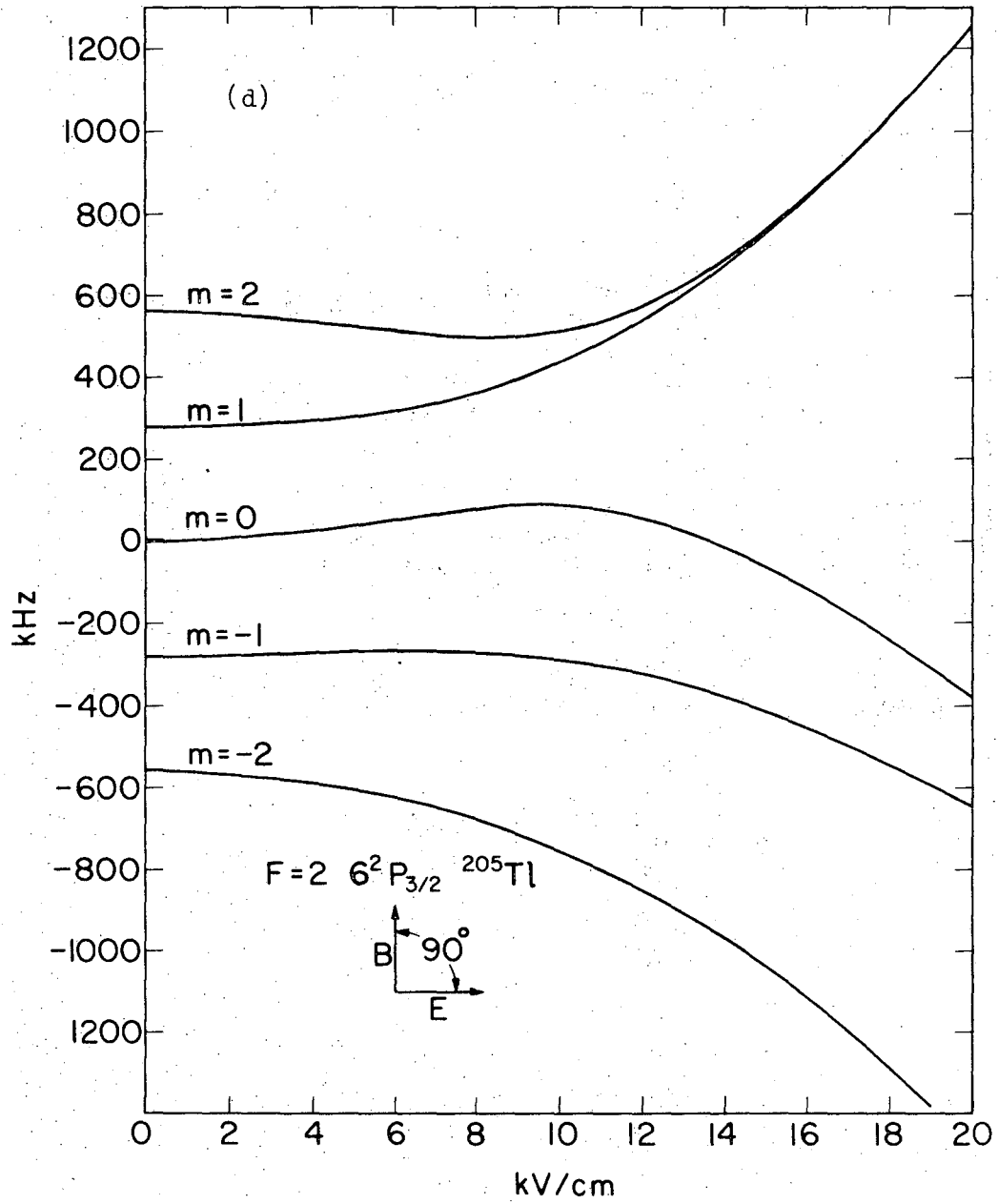
XBL703-2579

Fig. 3b



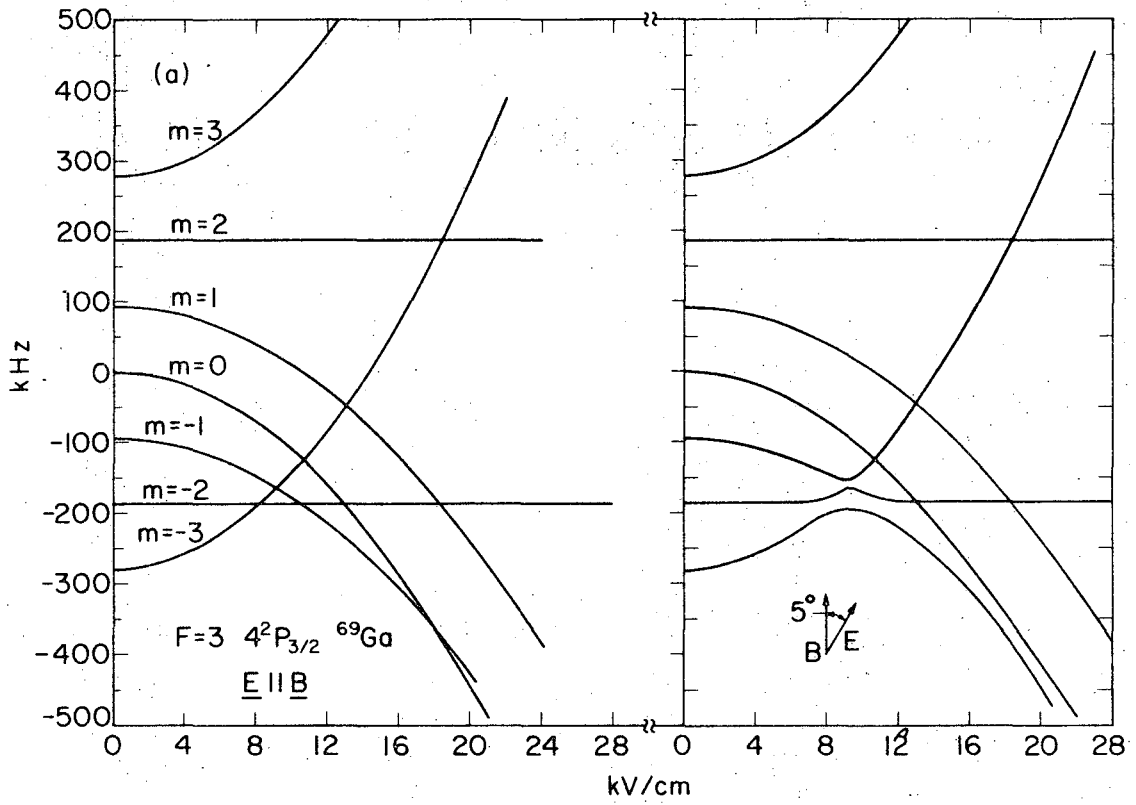
XBL703-2581

Fig. 3c



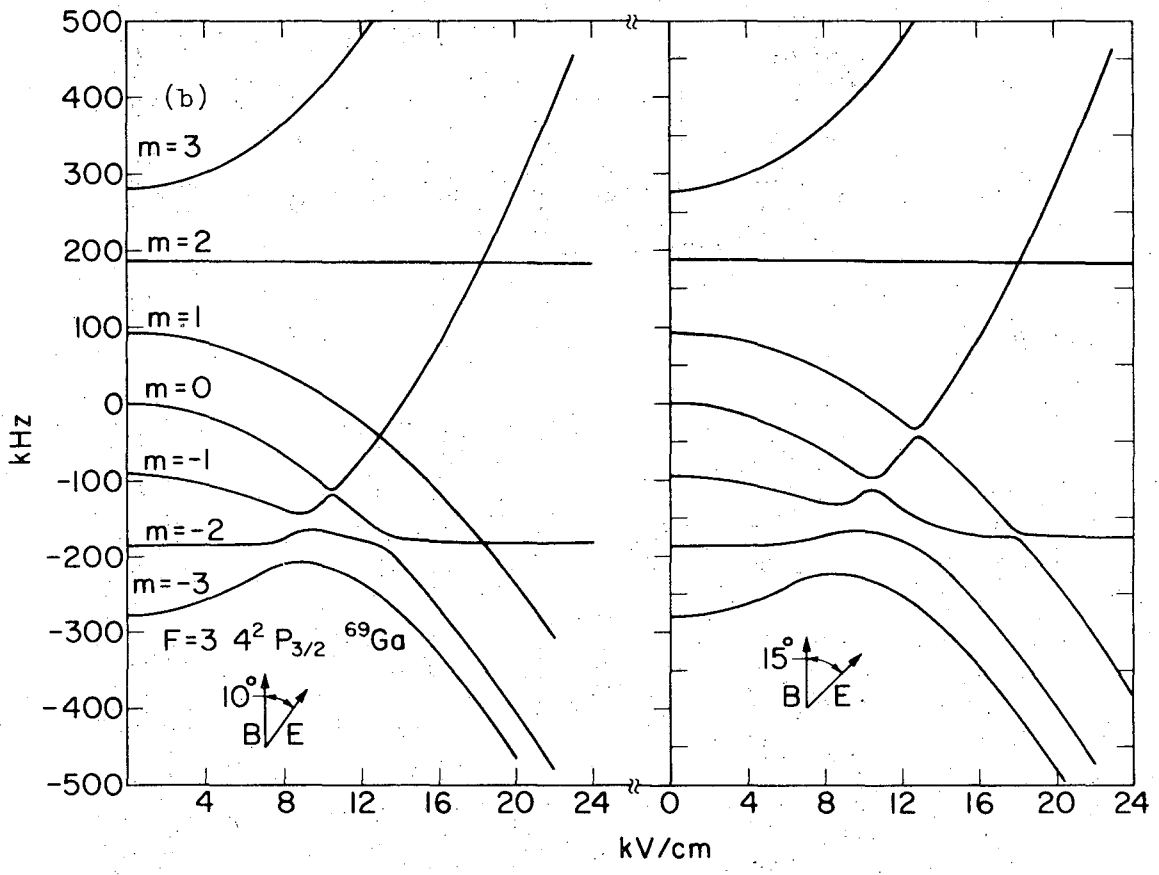
XBL703-2583

Fig. 3d



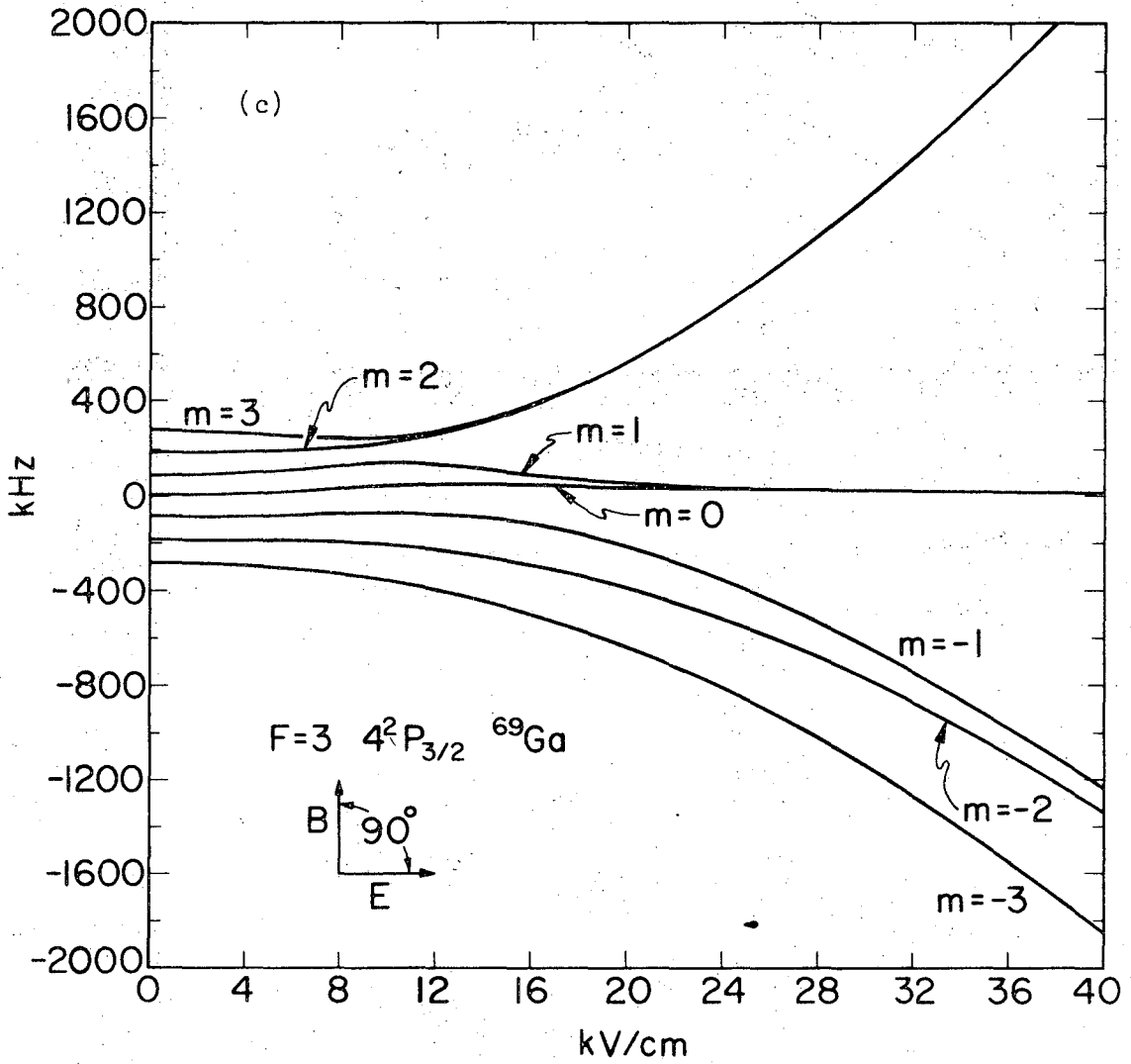
XBL703-2573

Fig. 4a



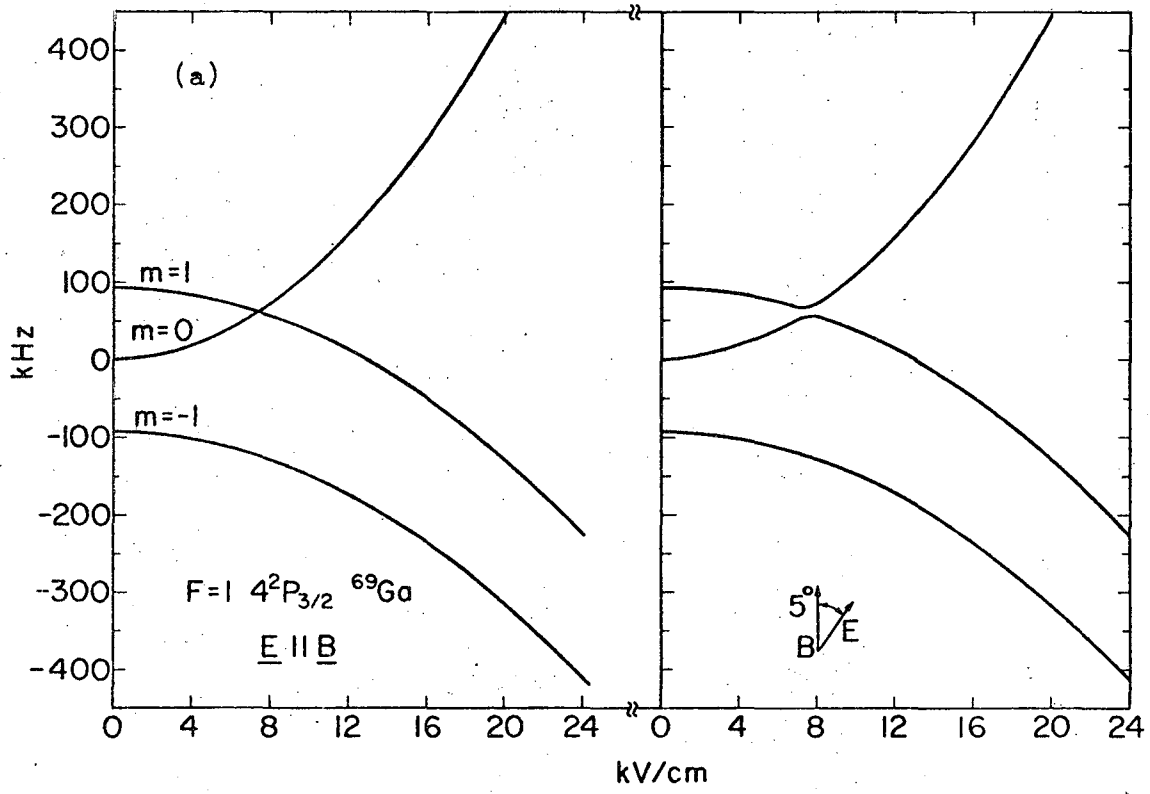
XBL703-2574

Fig. 4b



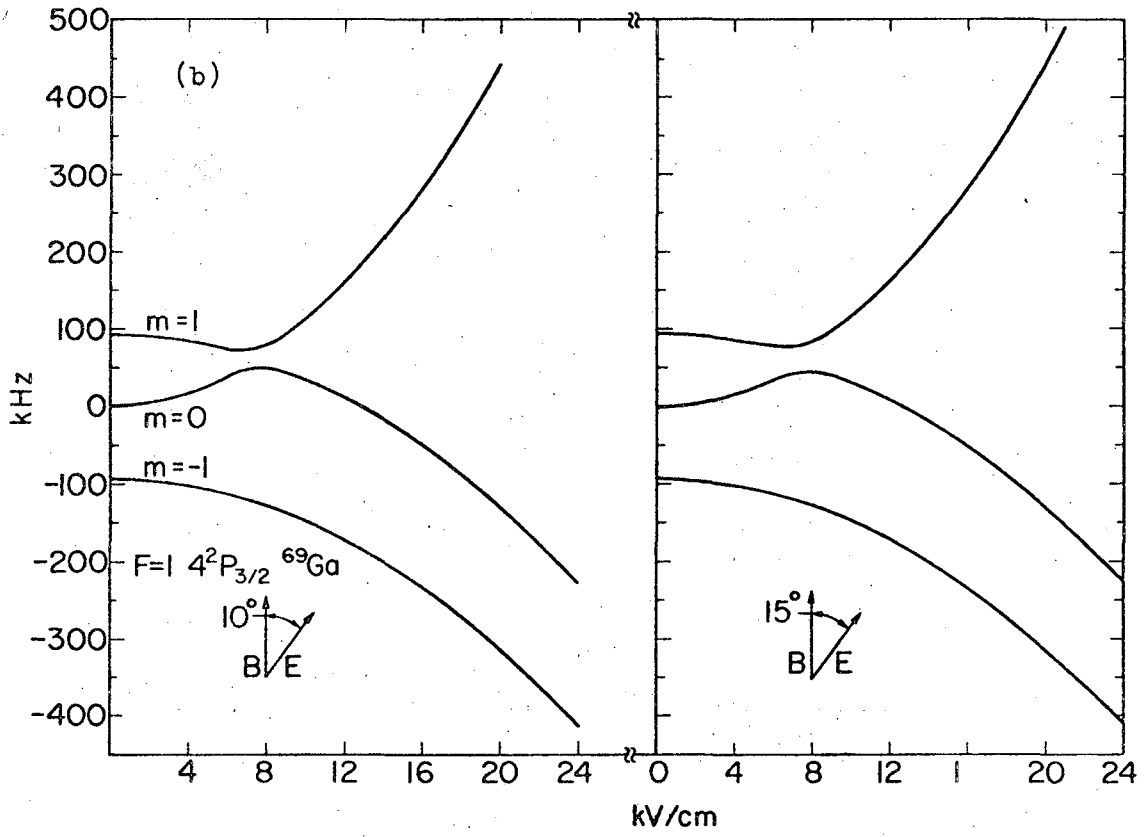
XBL703-2571

Fig. 4c



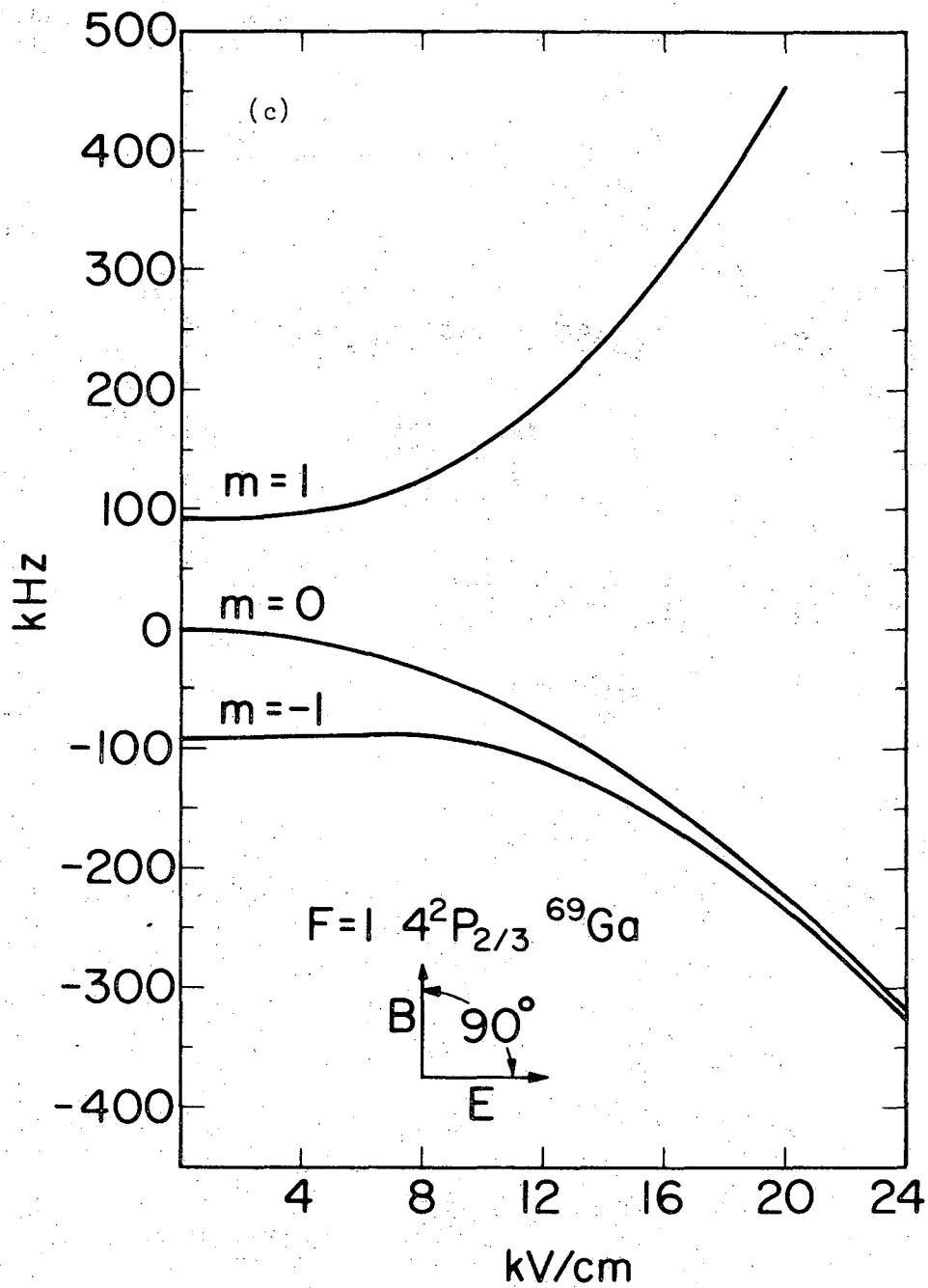
XBL703-2568

Fig. 5a



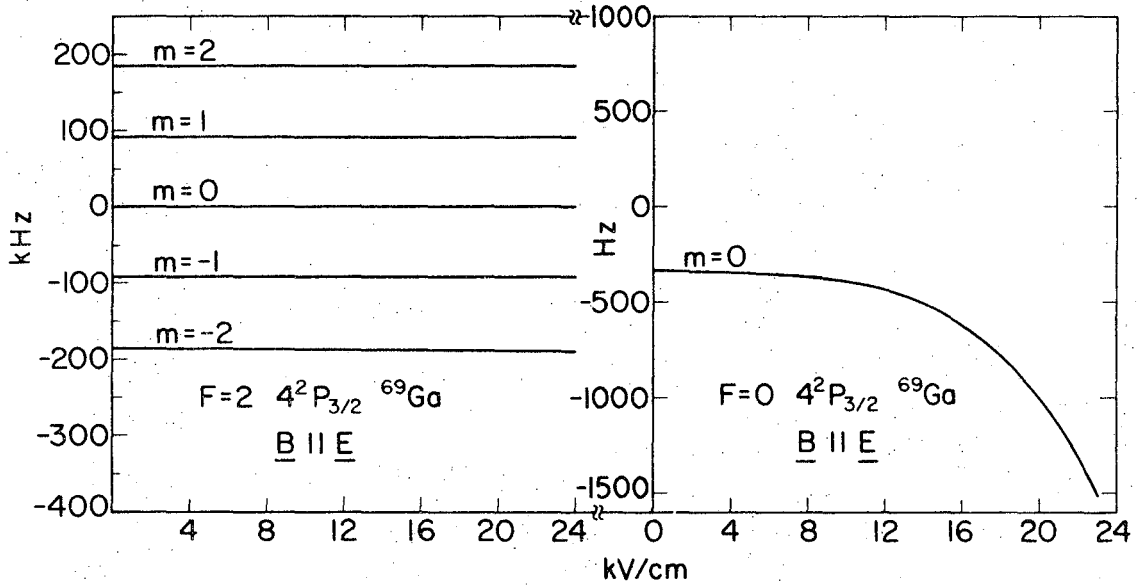
XBL703-2569

Fig. 5b



XBL703-2570

Fig. 5c



XBL703-2572

Fig. 6

LEGAL NOTICE

This report was prepared as an account of Government sponsored work. Neither the United States, nor the Commission, nor any person acting on behalf of the Commission:

- A. Makes any warranty or representation, expressed or implied, with respect to the accuracy, completeness, or usefulness of the information contained in this report, or that the use of any information, apparatus, method, or process disclosed in this report may not infringe privately owned rights; or*
- B. Assumes any liabilities with respect to the use of, or for damages resulting from the use of any information, apparatus, method, or process disclosed in this report.*

As used in the above, "person acting on behalf of the Commission" includes any employee or contractor of the Commission, or employee of such contractor, to the extent that such employee or contractor of the Commission, or employee of such contractor prepares, disseminates, or provides access to, any information pursuant to his employment or contract with the Commission, or his employment with such contractor.

TECHNICAL INFORMATION DIVISION
LAWRENCE RADIATION LABORATORY
UNIVERSITY OF CALIFORNIA
BERKELEY, CALIFORNIA 94720